Analysis of Gait and Mechanical Property of Wall-climbing Caterpillar Robot

Kun Wang
Key Laboratory of Fundamental Science for National Defense, Novel Inertial Instrument and Navigation System Technology, School of Instrumentation Science and Opto-electronics Engineering, BeiHang University, Beijing 100191, P.R. China.
Email: wangkunggg@163.com

Wei Wang
School of Mechanical Engineering and Automation, BeiHang University, Beijing 100191, China
Email: wangweilab@buaa.edu.cn

Houxiang Zhang
TAMS, Department of Informatics University of Hamburg Vogt-Kölln-Straße 30, Hamburg 22527, Germany.
Email: hzhang@informatik.uni-hamburg.de

***Abstract*—In order to demonstrate the validity and the benefit of the closed-chain kinematics of four-link motional method for the gait of wall-climbing caterpillar robot, the mathematical model and the relation of kinematical parameters were built. The caterpillar robot can climb on the wall by coordinated rotation of one active joint and three passive joints. The mechanical property of the closed-chain kinematics of four-link method is analyzed. And the relation of the driving joint torque and joint angle in wall-climbing process is deduced based on coplanar arbitrary force system. The coordinated control of multiple joints and the basis for selecting driving joints were discussed for developing the wall-climbing caterpillar robot. To testify the availability of the closed-chain kinematics of four-link method, a prototype of wall-climbing caterpillar robot with three kinds of adhesion modules based on vibrating suction method is designed. A successful wall-climbing test confirms both the principles of the closed-chain kinematics of four-link method and the validity of the adhesion modules based on vibrating suction method. The results show that the basis for selecting driving joints was reasonable and that the adhesion module based on vibrating suction method can produce powerful adsorption force with small weight and volume to ensure the safety and reliability of wall-climbing.**

***Index Terms*—four-link motional method, wall-climbing robot, mechanical property, vibrating suction method**

I. INTRODUCTION

Wall-climbing robot is a kind of special mobile robot, which can move and work on vertical wall to complete given tasks[1-5]. Although wall-climbing robots have been researched for many years, few practicable wall-climbing robots have been developed to perform very risky works. This is owing to two main difficulties in wall-climbing robot design: (1) Flexibility is in contradiction with weight. Heavy weight will counteract flexibility of the robot. Contrarily, wall-climbing robot with high flexibility can't be too much heavy; (2) Developing a simple mechanism, which have high degree of freedom (DOF) and can complete simple climbing gait[6-9].

According to the two designing difficulties mentioned above, a wall-climbing caterpillar robot based on a modular idea is proposed. Multi-joints mechanism makes the robot have high DOF but light weight. The modular wall-climbing caterpillar robot has a reconfigurable structure, higher flexibility and a lighter weight compared with traditional wall-climbing robots with multi-legs, sliding frame, wheeled and chain-track kinematics.

So far, snake robot is most similar to caterpillar robot in structure and motion gait. The first working snake robot was built by Professor S. Hirose in Tokyo Institute of Technology in 1972[10]. This robot was limited to planar motion, but snake robots capable of 3-D motion have appeared more recently[11-16]. Together with the robots, mathematical models of both the kinematics and the dynamics of snake robots have also been developed. In 2008, a new snake robot, which capable of planar obstacle avoiding and 3-D motion freely, was developed by Transeth in Norwegian University of Science and Technology (NTNU)/SINTEF Advanced Robotics Laboratory[17-19]. This robot is composed of several rigid joints which have two DOF. Transeth developed mathematical models of the dynamics of the snake robot precisely on the theory of Non-smooth Dynamical Systems. In 2001, the first snake robot in China is developed by five postgraduate students in National University of Defense Technology[20][21]. After that, some dexterous snake robots were built at both Shen Yang Institute of Automations and Shanghai Jiaotong University[22-24]. And the detailed mathematical model of the kinematics and the dynamics has also been developed. Comparatively speaking, the development of snake robot is more mature. And the serpentine motion of

doi:10.4304/jcp.7.3.706-715

the snake is much similar to the crawl of the caterpillar. Therefore, the control method and the gait of snake robot provide great reference value for the research of wall-climbing caterpillar robot. However, due to the constraint induced by the suction cups which attached on the wall, the wall-climbing caterpillar robot will be different from the snake robot in the following respects:

(1) Difference in the locomotion driving force. The snake robot mainly creeps on the ground, and its locomotion depends on the friction between the body and the ground. While the wall-climbing caterpillar robot works on the vertical wall. Because its locomotion driving force comes from the fixed constraint, the caterpillar robot must adsorb on the wall, or it will drop. Furthermore, the requirements of the driving joints were greatly enhanced due to the gravity of the robot. The driving joints not only need to rotate precisely in accordance with the programmed algorithm, but also need to compensate the impact of internal force caused by gravity and moment of inertia. Therefore, robust driving joints do become a basic condition for climbing wall successfully.

(2) Difference in the gaits and the control method. Snake robot can adopt many gaits to creep on the ground such as serpentine, lateral rolling, sinus-lifting, etc, while caterpillar robot only can crawl in vermicular motion. Snake robot can also adopt many control methods such as Central Pattern Generator (CPG) method[25], Obstacle-Aided[17][26] and Non-smooth Dynamical Systems[18][19][27], etc. In the beginning, caterpillar robot only adopted simple periodic control. Some mature caterpillar robot prototype, which adopted CPG method, began to appear with further research[28][29].

(3) Difference in the mechanism. Wall-climbing caterpillar robot needs adhesion modules to adsorb on the vertical wall, while snake robot dose not.

In a word, the robust driving joints, the proper control method and the reliable adhesion modules become three key points to make wall-climbing caterpillar robot climb on the wall safely and steadily. According to these three key points mentioned above, a wall-climbing caterpillar robot prototype was developed based on the structure specificity, the function of the robot, previous research experience and bionics. The paper is organized as follows. Section II gives an introduction for Four-links Motional Method (FMM). Through this method, the kinematical parameters of several passive joints can be determined by the rotation of one active joint. In order to give a theoretical basis for selecting driving joints, the mechanical property of FMM is analyzed. And the mechanical property simulation of FMM is given. In Section III, a new caterpillar robot prototype based on vibrating suction method is developed. The principle of the vibrating suction method[30][31] is not the research emphasis in this paper. So only the mechanism of the adhesion module is discussed, but not the reason why the adhesion module can adsorb on the wall. The experimental validation is given in Section IV. To simplify analysis, the caterpillar robot climbs on a glass wall in a longitudinal plane with no turning. The conclusions and suggestions for future work can be found in Section V.

II. Mechanical Property of Driving Joints

In previous research work[32], a simple caterpillar robot based on bionics was developed to study on the mechanism configuration and the climbing gait. After a serious experiment, the mechanism configuration of the caterpillar robot was concluded as shown in Fig. 1 and the climbing gait was confirmed as shown in Fig. 2.

Although the mechanism configuration of the caterpillar robot is much similar to the mechanism configuration of snake robot, the request of driving joints is much different. Snake robot creeps on the ground. The forces applied to every joint only come from adjacent links, and more or less uniform distribution. While because of gravity and moment of inertia, some joint maybe endured most complex load of the caterpillar robot in some dangerous state. It is necessary to analyze the mechanical property of driving joints to choose a robust joint for that the proper driving joints is a key point to make the caterpillar robot climb on the wall successfully. The proposition of the mechanism configuration of the caterpillar robot[32] is not discussed in this Section. In this Section, It is emphatically analyzed that how the joints rotate coordinately to make the robot climb on the wall and how the mechanical property of driving joints be analyzed to deduce the theoretical basis for selecting driving joints.

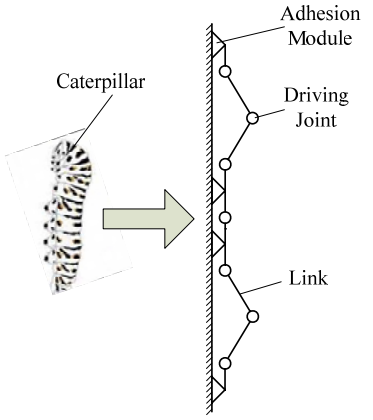

Figure 1. The configuration of the wall-climbing caterpillar robot.

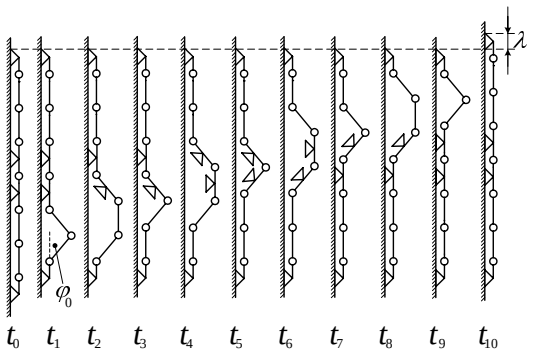

Figure 2. The gait of wall-climbing caterpillar robot.

A. Kinematics Analysis of FMM

Fig. 2 depicts the gait of wall-climbing caterpillar robot. And λ is the step length, which is generated in one cycle motion. As shown in Fig. 2, the caterpillar robot motion can be regarded as the multi-links motion.

Process t_0~t_1 and t_9~t_{10} are open-chain motion. And the head or tail suction cup can be controlled by 3 joints to move in longitudinal plane with 3 DOF. In open-chain motion process, a simple control method which called Unsymmetrical Phase Method[33] was adopted. So the discussion of open-chain control method is omitted here. Process t_1~t_9 is closed-chain motion of trunk. And there are only 4 rotating joints in instantaneous time. The effect of the suction cups deformation on the caterpillar robot is omitted for simplified analysis. So the motion of both joints and links of trunk in instantaneous time can be simplified as four-link motion. There is only 1 DOF in the four-link motion, but 4 rotating driving joints exist in instantaneous time. So these 4 driving joints must be divided into 1 active joint and 3 passive joints. Or redundant actuation will occur.

Only head suction cup and tail suction cup absorbing on the wall as t_4, t_5 and t_6 shown in Fig. 2. And the driving force of every driving joint in these three dangerous states might be bigger than that in other states. Process t_3~t_5 as a research object will be analyzed to deduce the kinematical relation between active joint and passive joints. There are two reasons for choosing process t_3~t_5 as the research object:

(1) The shape of the caterpillar robot at t_4 is much similar to the shape at t_6 except that the wave of the caterpillar robot at t_6 is higher one link length than the wave at t_4. While this length of one link is just produced in process t_3~t_5.

(2) The caterpillar robot begin to change open-chain to closed-chain at t_3. And all gravity of the robot is applied on the head suction cup and the tail suction cup. So the internal force of all the driving joints might be the maximum.

Ignore the impact caused in the transition of the kinematical chain. Therefore the process t_3~t_5 is a special case of the gait.

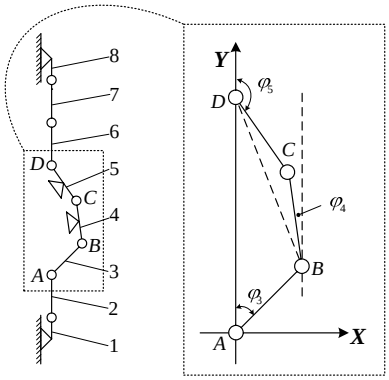

Figure 3. The instantaneous state of the caterpillar robot in process t_3~t_5.

Fig. 3 (left) depicts the instantaneous state of the caterpillar robot in process t_3~t_5. The links (modules) of the robot were numbered 1~8 from bottom to top. And the rotating joints were numbered *A*, *B*, *C* and *D*. Let the inertial reference frame be approximated by an earth-fixed frame I={*A*, *X*, *Y*} with the origin *A* attached to the joint *A* as shown in Fig. 3 (right). Let AB=BC=CD=l and $AD=\tilde{l}=(1+2\cos\varphi_0)l$, where φ_0 is the initial angle as shown in Fig. 2 (t_2). A general notation used in this paper is that an angle from the link i to the positive *Y*-axis direction of I is given by φ_i ($0^o \leqslant \varphi_i \leqslant 180^o$). And the sign of φ_i is determined by left-hand rule. For example, as the Fig. 3 shows now, φ_3 is positive, φ_4 is negative and φ_5 is positive. So the following equation can be deduced through the geometric relation of the links:

$$\begin{cases} l\cos\varphi_3 = y_B \\ l\sin\varphi_3 = x_B \\ l\cos\varphi_4 = y_C - y_B \\ l\sin\varphi_4 = x_C - x_B \\ l\cos\varphi_5 = y_C - \tilde{l} \\ l\sin\varphi_5 = x_C \end{cases} \tag{1}$$

Let $\varpi_3 = \varphi_3'$ be the angular velocity of *AB* and $\varepsilon_3 = \varphi_3''$ be the angular acceleration of *AB* when they exist. Let v_{Bx} and v_{By} be the two velocity component of joint *B*. And let a_{Bx} and a_{By} be the two acceleration component of joint *B*. Then the angular velocity (ϖ_4, ϖ_5) and the angular acceleration (ε_4, ε_5) of *BC* and *CD* can be deduced according to both the relation of vectors ($\overrightarrow{AC} = \overrightarrow{AB} + \overrightarrow{BC} = \overrightarrow{AD} + \overrightarrow{DC}$) and the velocity composition theorem.

$$\begin{cases} \varpi_4 = \dfrac{-v_{Bx}x_C - v_{By}(y_C - \tilde{l})}{x_C(y_C - y_B) - (y_C - \tilde{l})(x_C - x_B)} \\ \varpi_5 = \dfrac{-v_{Bx}(x_C - x_B) - v_{By}(y_C - y_B)}{x_C(y_C - y_B) - (y_C - \tilde{l})(x_C - x_B)} \end{cases} \tag{2}$$

$$\begin{cases} \varepsilon_4 = \dfrac{E\cdot(y_C - \tilde{l}) + F\cdot x_C}{(x_C - x_B)(y_C - \tilde{l}) - x_C(y_C - y_B)} \\ \varepsilon_5 = \dfrac{E\cdot(y_C - y_B) + F\cdot(x_C - x_B)}{(x_C - x_B)(y_C - \tilde{l}) - x_C(y_C - y_B)} \end{cases} \tag{3}$$

Where:

$$E = -a_{Bx} - \varpi_4^2(y_C - y_B) + \varpi_5^2(y_C - \tilde{l}) \tag{4}$$

$$F = -a_{By} + \varpi_4^2(x_C - x_B) + \varpi_5^2 x_C \tag{5}$$

$$v_{Bx} = \omega_3 l\cos\varphi_3 = \omega_3(y_B - y_A) \tag{6}$$

$$v_{By} = -\omega_3 l\sin\varphi_3 = -\omega_3(x_B - x_A) \tag{7}$$

$$a_{Bx} = -\omega_3^2(x_B - x_A) + \varepsilon_3(y_B - y_A) \quad (8)$$

$$a_{By} = -\omega_3^2(y_B - y_A) - \varepsilon_3(x_B - x_A) \quad (9)$$

According to Eq. (1)~(9), kinematical parameters such as ϖ_3, ϖ_4, ϖ_5, ε_3, ε_4 and ε_5 can be deduced if φ_3 is given. And this makes the gait planning very convenient. The kinematical parameters of joint *B*, joint *C* and joint *D* can be decided by the angle function of joint *A* when compile program. Here, joint *A* is regarded as active joint and joint *B*, joint *C*, joint *D* are regarded as passive joints. Joint *B*, joint *C* and joint *D* will be used as active joints in turn for transferring wave upward until the wave is transferred to the head of the caterpillar robot. Then the closed-chain is over.

B. Mechanical Analysis

The mechanical analysis in this Section is for torque solution of active joint in Section II.C. It is necessary to explain the concept of *Proportional Coefficient of Center of Gravity* (k_i) firstly. Every module of caterpillar robot is simplified as a link with fixed center of gravity for simplified analysis. Define the joint *i* be the joint which between link *i* and link *i*+1. Let L_i (*i*=1, 2,…, 8) be the length of every link, where $L_i=l$ (*i*=2, 3,…, 7). Other parameters can be defined as mass m_i, center of gravity Q_i and proportional coefficient of center of gravity k_i. Therefore k_i can be defined as the ratio of the length between Q_i and joint *i*-1 and L_i, as shown in Fig. 4.

Fig. 5 depicts schematic diagram of mechanical analysis in instantaneous state of the caterpillar robot in process t_3~t_5 (as shown in Fig. 2). And the earth-fixed frame is identical with frame *I* as shown in Fig. 3.

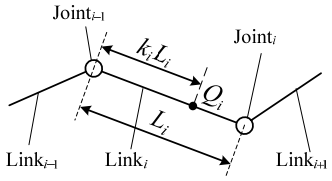

Figure 4. The schematic diagram of k_i.

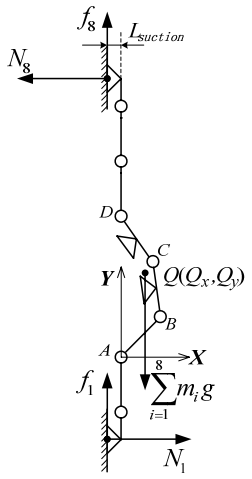

Figure 5. Schematic diagram of mechanical analysis.

Let $L_{suction}$ be the height of the suction cup, f_1 be the friction between link 1 (tail suction cup) and contact surface, f_8 be the friction between link 8 (head suction cup) and contact surface, N_1 be the supporting force of contact surface to link 1 (tail suction cup), N_8 be the supporting force of contact surface to link 8 (head suction cup), $Q(Q_x, Q_y)$ be the instantaneous center of gravity of the caterpillar robot. Because the characteristics and contact states of both head suction cup and tail suction cup are all identical, the following equation can be obtained:

$$f_1 = f_8 = \frac{1}{2}\sum_{i=1}^{8} m_i g \,.$$

The center of gravity can be obtained by following equation:

$$Q_x = \frac{\sum_{i=1}^{8} Q_{ix} m_i}{\sum_{i=1}^{8} m_i} = \frac{m_3 k_3 x_B + m_4[(1-k_4)x_B + k_4 x_C] + m_5(1-k_5)x_C}{\sum_{i=1}^{8} m_i} \quad (10)$$

Eq. (11) and Eq. (12) can be obtained by the equilibrium condition of forces in Fig. 5.

$$(Q_x + L_{suction})\sum_{i=1}^{8} m_i g = N_8 \cdot (L_1 + L_8 + 3l + \tilde{l}) \quad (11)$$

$$N_1 - N_8 = 0 \quad (12)$$

So N_1 and N_8 can be obtained by Eq. (11) and (12):

$$N_1 = N_8 = \frac{Q_x + L_{suction}}{L_1 + L_8 + 3l + \tilde{l}} \cdot \sum_{i=1}^{8} m_i g \quad (13)$$

C. Torque Solution of Active Joint

There is only 1 DOF in four-link motion. While four driving joints rotate in same time in the wall-climbing process. In order to avoid redundant actuation, these four rotating driving joints must be divided into 1 active joint and 3 passive joints. In this Section, the state as shown in Fig. 5 will still be analyzed. Because this is a dangerous state in the wall-climbing gait and joint *A* maybe endured maximum complex load from other links of caterpillar robot. Joint *B*, joint *C* and joint *D* are passive joints and they rotate to go with the rotation of active joint *A*. Therefore joint *B*, joint *C* and joint *D* can be regarded as hinges. That means there is no torque to produce in these 3 passive joints. The joints with no rotation (such as joint 1, joint 6 and joint 7) can be regarded as rigid connection. So the instantaneous motion of caterpillar robot is equivalent to the instantaneous four-link motion. Detail analysis will be given as follows.

Fig. 6 depicts the mechanical analysis of link 6, link 7 and link 8.

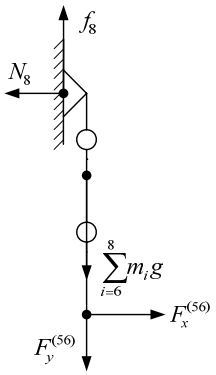

Figure 6. Mechanical analysis of link 6, link 7 and link 8.

Eq. (14) and (15) can be obtained through instantaneous equilibrium condition of forces.

$$F_x^{(56)} = \frac{Q_x + L_{suction}}{L_1 + L_8 + 3l + \tilde{l}} \cdot \sum_{i=1}^{8} m_i g \tag{14}$$

$$F_y^{(56)} = f_8 - \sum_{i=6}^{8} m_i g = \frac{1}{2}\sum_{i=1}^{8} m_i g - \sum_{i=6}^{8} m_i g \tag{15}$$

Fig. 7 depicts the mechanical analysis of link 5 (link *CD* as shown in Fig. 5).

Let joint *D* be the rotation axis. So Eq. (16) and (17) can be obtained through theorem of inertia moment and formula of centripetal force.

$$F_x^{(45)} = \frac{m_5 g k_5 x_C \cos\varphi_5}{x_C \sin\varphi_5 + (y_C - \tilde{l})\cos\varphi_5} - \frac{m_5 l(1-k_5)[(y_C - \tilde{l})(1-k_5)\varepsilon_5 + x_C\varpi_5^2]}{x_C \sin\varphi_5 + (y_C - \tilde{l})\cos\varphi_5} + \frac{F_x^{(65)} x_C \sin\varphi_5 - F_y^{(65)} x_C \cos\varphi_5}{x_C \sin\varphi_5 + (y_C - \tilde{l})\cos\varphi_5} \tag{16}$$

$$F_y^{(45)} = -\frac{m_5 g[(y_C - \tilde{l})\cos\varphi_5 + (1-k_5)x_C \sin\varphi_5]}{x_C \sin\varphi_5 + (y_C - \tilde{l})\cos\varphi_5} + \frac{m_5 l(1-k_5)[(y_C - \tilde{l})\varpi_5^2 - (1-k_5)x_C\varepsilon_5]}{x_C \sin\varphi_5 + (y_C - \tilde{l})\cos\varphi_5} + \frac{(y_C - \tilde{l})[F_y^{(65)}\cos\varphi_5 - F_x^{(65)}\sin\varphi_5]}{x_C \sin\varphi_5 + (y_C - \tilde{l})\cos\varphi_5} \tag{17}$$

Fig. 8 depicts the mechanical analysis of link 4 (link *BC* as shown in Fig. 5).

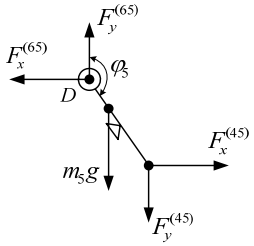

Figure 7. Mechanical analysis of link 5.

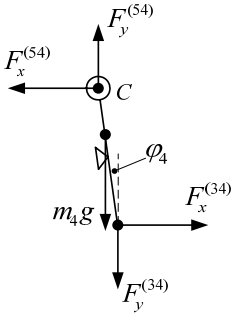

Figure 8. Mechanical analysis of link 4.

Let joint *C* be the rotation axis. So Eq. (18) and (19) can be obtained through theorem of inertia moment and formula of centripetal force.

$$F_x^{(34)} = \frac{m_4 g k_4 (x_C - x_B)\cos\varphi_4}{(x_C - x_B)\sin\varphi_4 + (y_C - y_B)\cos\varphi_4} + \frac{m_4 l(1-k_4)[(x_C - x_B)\varpi_4^2 + g(1-k_4)(y_C - y_B)\varepsilon_4]}{(x_C - x_B)\sin\varphi_4 + (y_C - y_B)\cos\varphi_4} + \frac{(x_C - x_B)(F_x^{(54)}\sin\varphi_4 - F_y^{(54)}\cos\varphi_4)}{(x_C - x_B)\sin\varphi_4 + (y_C - y_B)\cos\varphi_4} \tag{18}$$

$$F_y^{(34)} = -\frac{m_4 g[(x_C - x_B)(1-k_4)\sin\varphi_4 + (y_C - y_B)\cos\varphi_4]}{(x_C - x_B)\sin\varphi_4 + (y_C - y_B)\cos\varphi_4} - \frac{m_4 l(1-k_4)[(y_C - y_B)\varpi_4^2 - g(1-k_4)(x_C - x_B)\varepsilon_4]}{(x_C - x_B)\sin\varphi_4 + (y_C - y_B)\cos\varphi_4} - \frac{(y_C - y_B)(F_x^{(54)}\sin\varphi_4 - F_y^{(54)}\cos\varphi_4)}{(x_C - x_B)\sin\varphi_4 + (y_C - y_B)\cos\varphi_4} \tag{19}$$

Fig. 9 depicts the mechanical analysis of link 3 (link *AB* as shown in Fig. 5).

Let joint *A* be the rotation axis. So the theoretical active joint torque *M* can be obtained through theorem of inertia moment.

$$M = m_3 l^2 k_3^2 \varepsilon_3 + m_3 g k_3 x_B - F_x^{(43)} y_B - F_y^{(43)} x_B \tag{20}$$

$F_*^{(jk)}$ and $F_*^{(kj)}$ is a pair of action and reaction force in Eq. (14) ~ (20) where * described in $F_*^{(jk)}$ and $F_*^{(kj)}$ denotes the *X*-axis or *Y*-axis. The theoretical torque of active joint can be calculated by Eq. (20). So a proper driving joint can also be selected theoretically.

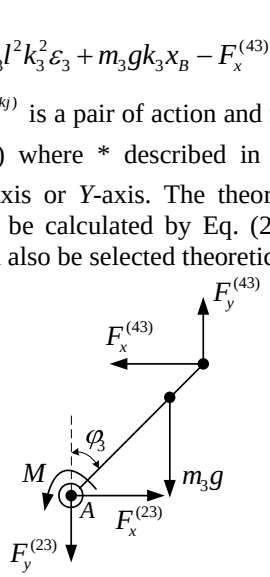

Figure 9. Mechanical analysis of link 3.

D. Torque Simulation of Active Joint

As the analysis mentioned above, a theoretical Eq. (20) was deduced for calculating the torque of active joint. Because of the existing mechanical and control errors, Eq. (20) can not be used directly for developing the caterpillar robot. Considering safety and reliability, the theoretical torque calculated by Eq. (20) must be multiplied by a safety factor for compensating the mechanical and control errors. Therefore, the torque simulation of active joint must be implemented before developing the caterpillar robot prototype.

Because of mechanical and control errors, variable complex load maybe applied to active joint in actual wall-climbing motion. And the variable complex load is hard to calculate precisely at present because of poor experimental conditions. Errors were not involved in Eq. (20). So it is necessary to multiply the theoretical torque, which is calculated by Eq. (20), by a proper safety factor for both compensating the effect of errors on the caterpillar robot motion and ensuring the wall-climbing motion successfully. Fig. 10 depicts the theoretical torque simulation of active joint.

The solid line as shown in Fig. 10 denotes the theoretical torque simulation of active joint *A* in process t_3~t_5 (as shown in Fig. 2). The dashed line denotes the angle of active joint *A* (φ_3 , the angle of link *AB*) changing with time. Let φ_3 change with uniform angular velocity for simplified analysis. And φ_3 change with following equation:

$$\varphi_3 = \begin{cases} 30 + \dfrac{5.2t}{180} & [0,180] \\ 35.2 - \dfrac{35.2(t-181)}{668} & [181,849] \end{cases} \quad (21)$$

As the Fig. 10 shows, a peak of theoretical torque *M* occurred at *t*=181 ms. The reason is that φ_3 changed its rotation direction, which leads to an infinite angular acceleration and infinite theoretical driving torque. This situation can not happen in actual wall-climbing motion but only an instantaneous maximum driving torque.

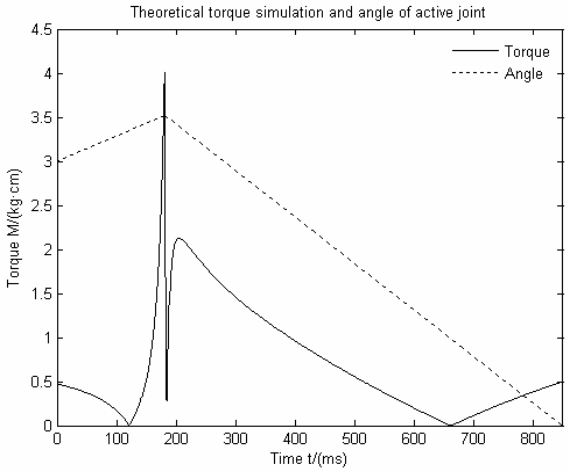

Figure 10. Theoretical torque simulation of active joint.

An additional statement should be announced: the curve of theoretical torque *M* as shown in Fig. 10 has already been revised a little. The peak of theoretical torque *M* in original simulation image (not Fig. 10) can reach to 7.86×10^{12} kgcm, which is 12 order of magnitude higher than the peak as shown in Fig. 10. In order to conform to reality more and observe conveniently, several torque value, which are too high to conform to reality, were omitted from original simulation image.

The maximum driving torque value is about 4 kgcm as shown in Fig. 10. And the torque value in other most time is less than 2 kgcm. In order to ensure the safety of wall-climbing motion, a quasi safety factor should not less than 3.5. So the rated torque of active driving joint should not less than 14 kgcm.

A conclusion can be obtained from the analysis above: That the sufficient adsorption force produced by head and tail suction cups and that the precise angle controlled by 1 active joint and 3 passive joints can both make the rotating joints move according with the four-link motion and make the caterpillar robot climb on the wall according with the gait as shown in Fig. 2. Therefore how to ensure that suction cups can produce sufficient adsorption force becomes the first problem need to be solved to make the caterpillar robot climb on the wall successfully. In Section III, the working principle of the adhesion module will be discussed. The adsorption principle adopted in this caterpillar robot is different from traditional passive adsorption. Objectively speaking, there is no direct relationship between the adsorption principle adopted in this caterpillar robot and the torque of active driving joint. So, in Section III, the mechanism principle of producing adsorption force will be discussed. And the adsorption principle[30][31], which is not the emphases in this paper, will not be involved.

III. Development of Caterpillar Robot

The adsorption function of wall-climbing robots is one of the most significant characteristics, which is different from the characteristic of mobile robots on the ground. There are two important problems need to be solved for mini wall-climbing robot. The one is that adequate adsorption force must be produced to ensure mini wall-climbing robots working on the wall safely and reliably. The other one is to avoid using a long trachea as much as possible to reduce the weight of wall-climbing robot. An adhesion module based on vibrating suction method[30][31] is developed according to the two important problems mentioned above. Fig. 11 depicts the kinematical mechanism diagram of the adhesion module. An eccentric wheel rotates to make two middle suction cups move up and down (vibration). The vibration of the two middle suction cups can be transmitted to two bilateral suction cups by two levers. So the four suction cups can adsorb on the contact surface with vibrating suction method with 180^o phase difference at the same time.

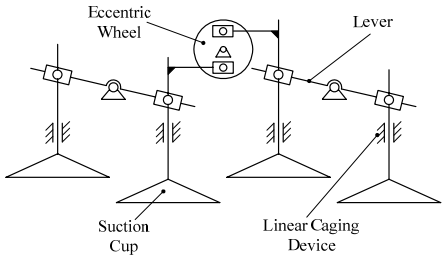

Figure 11. The kinematical schematic of mechanism of the adhesion module.

Fig. 12 depicts the schematic diagram of the adhesion module based on vibrating suction method (This Fig. shows an inner mechanism with no shell). The motor rotating or counter-rotating can make the module attach or detach the contact surface (the release mechanism was not shown in Fig. 12). The characteristics of this adhesion module are as follows:

(1) The mechanism is simple and compact. A small space was used reasonably and adequately. The volume of the whole adhesion module (with a shell) is 50 mm × 46 mm × 43 mm.

(2) That the adhesion module attaches or detaches the contact surface only needs one motor. So it saves a driving device.

(3) The adhesion module can attach or detach quickly and reliably.

(4) The power consumption of the adhesion module is low due to lubricate adequately.

A wall-climbing caterpillar robot, which according to FMM and the adhesion module mentioned above, was developed as shown in Fig. 13. And a one-to-one correspondence between the numbers 1~8 as shown in Fig. 13 and the numbers 1~8 as shown in Fig. 3 was presented.

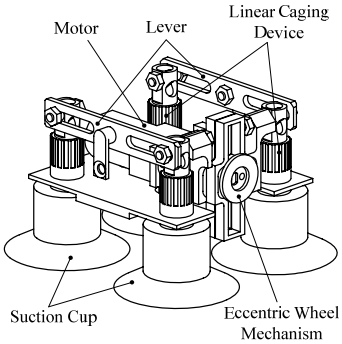

Figure 12. The schematic diagram of the adhesion module.

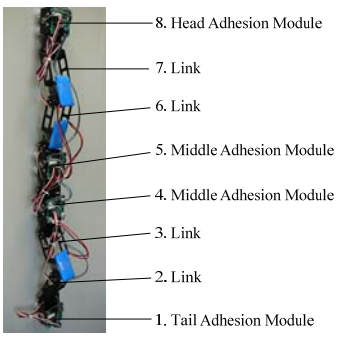

Figure 13. The prototype of the wall-climbing caterpillar robot.

In order to reduce the difficulty of both mechanism designing and control algorithm designing and also to reduce volume or weight of the robot, the lengths of link 2 ~ link 7 are designed equally besides link 1 (tail adhesion module) and link 8 (head adhesion module). Only self-tapping screws were adopted for assembling adjacent modules. This makes the robot assembly and disassembly very convenient. The design idea is beneficial to combine different modules and also beneficial to increase the amount of middle modules according to different working environment in order to improve wall-climbing safety and reliability. Servo motors (Model: hangood HG14-M) were adopted to be the driving joints. Table I describes some important parameters of caterpillar robot.

IV. Experiments

Absorption on the wall safely and reliably is one of the key points for wall-climbing robot climbing on the wall successfully. So in this experimental Section, the validity of the adhesion module based on vibrating suction method will be introduced firstly although the vibrating suction method is not the emphases in this paper. Secondly, the wall-climbing experiment of the caterpillar robot will be discussed.

A. Experiment About Adhesion Module

There are three kinds of adhesion module in the caterpillar robot: head adhesion module, tail adhesion module and middle adhesion module. The inner mechanism of these three kinds of adhesion module is same as shown in Fig. 12. Therefore only one kind of adhesion module needs to be verified. In this Section, the head adhesion module was adopted. The diameter of the suction cup is 30 mm. The material of the suction cup is silica.

The adhesion module experiment was carried out on four contact surfaces: cabinet surface, wooden door, office wall and glass surface. An additional statement should be announced: The suction cup can absorb on the glass surface safely even with no vibration. The purpose of making the suction cup absorbing on the glass surface with vibrating suction method is to compare with other three contact surfaces to increase the comparability of the

TABLE I.
PARAMETERS OF CATERPILLAR ROBOT

Parameters	Value
Whole length of the robot L/(mm)	750
Rated torque of active driving joint M/($kg \cdot cm$)	$\geqslant$14
Angle of active driving joint ϕ_i/(°)	$\pm$85
Length of tail adhesion module (link 1) L_1/(mm)	70
Length of head adhesion module (link 8) L_8/(mm)	80
Length of middle adhesion module (link 2~7) L_2~L_7/(mm)	100
Mass of tail adhesion module (link 1) m_1/(g)	112
Mass of head adhesion module (link 8) m_8/(g)	172
Mass of middle adhesion module (link 4~5) m_4, m_5/(g)	177
Mass of link 2, link 3, link 6 and link 7 m_2, m_3, m_6, m_7/(g)	90

adhesion module experiments. Fig. 14 are the experimental photos of head adhesion module absorbing on the cabinet surface, wooden door and office wall with same power consumption. Table II describes the experimental results.

B. Climbing Experiment of the Caterpillar Robot

The wall-climbing caterpillar robot was controlled to climb on the wall with the gait of FMM. And every joint rotated according to the relation between active joint and passive joints mentioned in the Section II. Adequate supporting force (N_1 and N_8 as shown in Fig. 5) must be produced by head and tail adhesion module in order to make the caterpillar robot motion accord with FMM more. That means no sliding of head and tail adhesion module was permitted to bring about. So the wall-climbing experiment was carried out on a glass wall because the adhesion module can produce bigger adsorption force on the glass contact surface than other three contact surfaces. Further to make the wall-climbing motion accord with FMM more.

Fig. 15 is a series of experimental photos of caterpillar robot climbing on the glass wall. And Fig. 15 depicts a whole periodic motion of process t_0~t_{10} and a step length λ generated in a cycle motion. A one-to-one correspondence between the numbers as shown in Fig. 15 and the numbers t_0~t_{10} as shown in Fig. 2 was presented. Table III describes some important results of caterpillar robot in wall-climbing experiment.

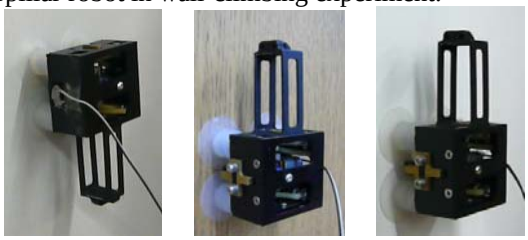

(a) Cabinet surface (b) Wooden door (c) Office wall

Figure 14. The prototype of the wall-climbing caterpillar robot.

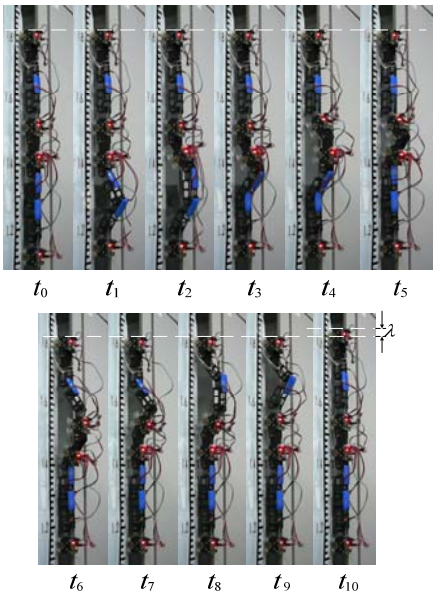

Figure 15. The experimental photos of caterpillar robot.

TABLE II.
EXPERIMENTAL RESULTS OF HEAD ADHESION MODULE

Contact surface	Parameters		
	Normal force F_x/(kg)	Tangential force F_y/(kg)	Power consumption p/(W)
Cabinet surface	1.4	0.8	0.48
Wooden door	1.7	1.0	0.48
Office wall	1.1	0.6	0.48
Glass surface	5.0	3.0	0.48

TABLE III.
RESULTS OF WALL-CLIMBING EXPERIMENT

Parameters	Value
Power consumption P/(W)	About 8
Climbing velocity v/(cm•min^{-1})	6.75
Initial angle ϕ_0/(°)	30
Step length λ/(cm)	2.7

The caterpillar robot climbed on the glass wall according to FMM mentioned in Section II-A. Every driving joint in closed-chain motion was used as active joint or passive joint in turn to transfer the wave upward. The wall-climbing experiment verified the validity and feasibility of that FMM can control the caterpillar robot to climb on the glass wall successfully. The wall-climbing experiment also verified the rationality of the basis mentioned in Section II-D for selecting a proper driving joint. But some problems emerged from the wall-climbing experiment of the caterpillar robot as follows:

(1) Three passive joints can not be completely regarded as hinges because of angle errors. And slight redundant actuation occurred in the wall-climbing motion.

(2) The internal force caused by driving joints in the wall-climbing motion applied to both the head and tail adhesion modules and increased the tangential movement tendency of the suction cups. This is harmful to the safety of the caterpillar robot although the deformation of the suction cups can eliminate some effect of the internal force which caused by driving joints.

(3) The vibration of adhesion modules made the base of the caterpillar robot unsteadiness and caused some disturbance to the caterpillar robot locomotion. That led driving joints to tremble in the process t_0~t_1 and process t_9~t_{10}.

V. CONCLUSIONS

(1) The closed-chain kinematics of Four-link Motional Method was proposed according to the gait of wall-climbing caterpillar robot.

(2) The mathematical model of FMM was built. And the angle relation between active joint and passive joints was deduced. The basis for selecting driving joints was derived by analyzing the mechanical property of driving joints in FMM.

(3) A wall-climbing caterpillar robot with adhesion module, which based on vibrating suction method, was

developed. Some absorption experiments were carried out in order to testify the validity of the adhesion module.

(4) A wall-climbing test for caterpillar robot was carried out according to FMM. And the validity and the benefit of FMM were testified theoretically. But the research work needs to be improved further because of some existing mechanical and control errors.

In future work, the research emphasis will focus on improving control precision of FMM both to achieve error compensation for passive joints and to algorithm optimization. The future research emphasis will also focus on how to reduce the unsteadiness of the base of caterpillar robot caused by vibration in the mechanical viewpoint.

ACKNOWLEDGMENT

This work was supported in part by a grant from National Natural Science Foundation of China (Grant No. 50605001) and National Hi-tech Research and Development Program of China (863 Program, Grant No. 2006AA04Z250).

REFERENCES

[1] Houxiang Zhang, Sky Cleaners[EB/OL].(2008-10-12). http://tams-www.informatik.uni-hamburg.de/people/hzhang/projects/skycleaners/

[2] Shanqiang Wu, Mantian Li, Shu Xiao, Yang Li, "A wireless distributed wall climbing robotic system for reconnaissance purpose", Proceedings of the 2006 IEEE International Conference on Mechatronics and Automation, Luoyang, China, June 25-28, 2006: 1308-1312.

[3] MIYAKE T, ISHIHARA H, YOSHIDA R S S, "Development of small-size window cleaning robot: a traveling direction control on vertical surface using accelerometer", Proceedings of the 2006 IEEE International Conference on Mechatronics and Automation, Luoyang, China, June 25-28, 2006: 1302 - 1307.

[4] Zhiyuan Qian, Yanzheng Zhao, Zhuang Fu, "Development of wall-climbing robots with sliding suction cups", Proceedings of the 2006 IEEE/RSJ International Conference on Intelligent Robots and Systems, Beijing, China, October 9-15, 2006: 3417 - 3422.

[5] Jizhong Xiao, MORRIS W, CHAKRAVARTHY N, "City-climber: a new generation of mobile robot with wall-climbing capability", Proceedings of the 2006 SPIE The International Society for Optical Engineering, Orlando (Kissimmee), FL, USA, April 17 2006, Vol. 6230 62301D-1.

[6] Houxiang Zhang, Jianwei Zhang, Rong Liu, Guanghua Zong, "Realization of a service robot for cleaning spherical surfaces", *International Journal of Advanced Robotic Systems*, 2005, 2 (1): 53-58.

[7] NISHI A, MIYAGI H, "A wall-climbing robot using propulsive force of a propeller: mechanism and control in a mild wind", *JSME international journal. Ser. C, Dynamics, control, robotics, design and manufacturing*, 1993, 36-C(3): 361-367.

[8] Daltorio, K.A., Witushynsky, T.C., Wile, G.D., Palmer, L.R., Malek, A.A., Ahmad, M.R., et al, "A body joint improves vertical to horizontal transitions of a wall-climbing robot", Proceedings of the 2008 IEEE International Conference on Robotics and Automation, Pasadena, CA, USA, May 19-23, 2008: 3046 - 3051.

[9] A. Saunders, M. Buehler, D. I. Goldman, R. J. Full, "The RiSE climbing robot: body and leg design", Proceedings of the 2006 SPIE The International Society for Optical Engineering, Orlando (Kissimmee), FL, USA, April 17 2006, Vol. 6230 623017-1.

[10] HIROSE S, MORI M. "Biologically inspired snake-like robots", Proceedings of the 2004 IEEE International Conference on Robotics and Biomimetics, Shenyang, China, August 22-26, 2004: 1-7.

[11] HIROSE S, MORISHIMA A. "Design and control of a mobile robot with an articulated body", *International Journal of Robotics Research*, 1990, 9 (2): 99–114.

[12] LILJEB¨ACK P, STAVDAHL Ø, PETTERSEN K Y. "Modular pneumatic snake robot: 3D modelling, implementation and control", Proceedings of the 16th IFAC World Congress, Prague, Czech Republic, July 2005.

[13] MORI M, HIROSE S. "Three-dimensional serpentine motion and lateral rolling by active cord mechanism ACM-R3", Proceedings of the 2002 IEEE/RSJ Int. Conference on Intelligent Robots and System, Lausanne, Switzerlan, October, 2002: 829–834.

[14] CHIRIKJIAN G, BURDICK J. "Design and experiments with a 3 DOF robot", Proceedings of the 1993 IEEE International Conference on Robotics and Automation, May 2-6, 1993, 3: 113–119.

[15] CHIRIKJIAN G, BURDICK J. "The kinematics of hyper-redundant robot locomotion", *IEEE Transactions on Robotics and Automatics*, Dec. 1995, 11 (6): 781–793.

[16] BURDICK J, RADFORD J, CHIRIKJIAN G. "A 'sidewinding' locomotion gait for hyper-redundant robots", Proceedings of the 1993 IEEE International Conference on Robotics and Automation, May 2-6, 1993, 3: 101–106.

[17] Aksel Andreas Transeth, Remco I. Leine, Christoph Glocker, Kristin Ytterstad Pettersen, P°al Liljeb¨ack, "Snake robot obstacle-aided locomotion: modeling, simulations, and experiments", *IEEE Transactions on Robotics*, 2008, 24 (1): 88-104.

[18] Aksel A. Transeth, Remco I. Leine, Christoph Glocker, Kristin Y. Pettersen, "3-D snake robot motion: nonsmooth modeling, simulations, and experiments", *IEEE Transactions on Robotics*, 2008, 24 (2): 361-376.

[19] Transeth, A.A., Leine, R.I., Glocker, C., Pettersen, K.Y., "Non-smooth 3D modeling of a snake robot with external obstacles", Proceedings of the 2006 IEEE International Conference on Robotics and Biomimetics, Kunming, China, December 17-20, 2006: 1189 - 1196.

[20] Daibing Zhang. Chinese first snake robot was born[EB/OL].(2001-11-27). http://www.chinamil.com.cn/gb/pladaily/2001/11/27/20011127001006.html. (in Chinese)

[21] Daibing Zhang. Chinese first snake robot was developed successfully by five young postgraduate students[EB/OL].(2002-01-15). http://www.chinamil.com.cn/gb/defence/2002/01/15/20020115017154_zhxw.html. (in Chinese)

[22] Changlong Ye, Shugen Ma, Bin Li, Hongjun Liu, Hequan Wang, "Development of a 3D snake-like robot: perambulator-II", Proceedings of the 2007 IEEE International Conference on Mechatronics and Automation, Harbin, China, August 5-8, 2007: 117-122.

[23] Shugen Ma, Ohmameuda, Y., Inoue, K., Bin Li, "Control of a 3-dimensional snake-like robot", Proceedings of the 2003 IEEE International Conference on Robotics and Automation, Taipei, Taiwan, September 14-19, 2003 (2): 2067–2072.

[24] Li Chen, Shugen Ma, Yuechao Wang, Bin Li, Dengping Duan, "Design and modelling of a snake robot in traveling

wave locomotion", *Mechanism and Machine Theory*, 2007, 42: 1632–1642.
[25] CRESPI A, IJSPEERT A J, "Online optimization of swimming and crawling in an amphibious snake robot", *IEEE Transactions on Robotics*, 2008, 24 (1): 75-87.
[26] TRANSETH A A, LILJEB¨ACK P, PETTERSEN K Y, "Snake robot obstacle aided locomotion: an experimental validation of a non-smooth modeling approach", Proceedings of the 2007 IEEE/RSJ International Conference on Intelligent Robots and Systems, San Diego, CA, USA, October 29- November 2, 2007: 2582-2589.
[27] Transeth A.A., Leine R.I., Glocker C., Pettersen K.Y., "Non-smooth 3D modeling of a snake robot with frictional unilateral constraints", Proceedings of the 2006 IEEE International Conference on Robotics and Biomimetics, Kunming, China, December 17-20, 2006: 1181-1188.
[28] Wei Wang, Yingying Wang, Kun Wang, Houxiang Zhang, Jianwei Zhang, "Analysis of the kinematics of module climbing caterpillar robots", Proceeding of 2008 IEEE/ASME International Conference on Advanced Intelligent Mechatronics, Xi'an, China, July 2-5, 2008: 84-89.
[29] Wei Wang, Yingying Wang, Jinghao Qi, Houxiang Zhang, Jianwei Zhang, "The CPG control algorithm for a climbing worm robot", Proceedings of the 3rd IEEE Conference on Industrial Electronics and Applications, Singapore, June 3-5, 2008: 675 - 679.
[30] Tao Zhu, Rong Liu, Xudong Wang, Kun Wang, "Principle and application of vibrating suction method", Proceedings of the 2006 IEEE International Conference on Robotics and Biomimetics, Kunming, China, December 17-20, 2006: 491-495.
[31] Kun Wang, Wei Wang, Dazhai Li, Guanghua Zong, Houxiang Zhang, Jianwei Zhang, et al, "Analysis of two vibrating suction methods", Proceedings of the 2008 IEEE International Conference on Robotics and Biomimetics, Bangkok, Thailand, February 21-26, 2009: 1313-1318.
[32] Wei Wang, Kun Wang, Houxiang Zhang, "Crawling gait realization of the mini-modular climbing caterpillar robot", *Progress in Natural Science* 19 (2009) 1821–1829
[33] Wei Wang, Houxiang Zhang, Kun Wang, "Gait control of modular climbing caterpillar robot", Proceeding of 2009 IEEE/ASME International Conference on Advanced Intelligent Mechatronics, Singapore, July 14-17, 2009.

Kun Wang was born in Yichun City, Heilongjiang Province, China on 1982. He received the M.Sc. degree from the Robotics Institute, School of Mechanical Engineering and Automation, BeiHang University(BUAA), Beijing, China, in 2007. The major was Mechanical Designing and Theory. He received the P.HD. degree from the Robotics Institute, School of Mechanical Engineering and Automation, BeiHang University(BUAA), Beijing, China, in 2010. The major was mechanical electronic engineering.

He is currently a Postdoctoral Researcher in the Key Laboratory of Fundamental Science for National Defense, Novel Inertial Instrument and Navigation System Technology, School of Instrumentation Science and Opto-electronics Engineering, BeiHang University, Beijing, China. His mainly work is mechanical design for high speed motor with magnetic bearing.